Journal of Applied Polymer Science

Characterization of nanocomposite resol resins: Individual/synergist effects of alendronic acid and sepiolite

Ümran Burcu Alkan,[1] Nilgün Kızılcan[1,2]
[1]Graduate School of Science Engineering and Technology Polymer Science and Technology Department, Istanbul Technical University, Istanbul 34469, Turkey
[2]Faculty of Science, Department of Chemistry, Istanbul Technical University, Istanbul 34469, Turkey
Correspondence to: N. Kızılcan (E-mail: kizilcan@itu.edu.tr)

ABSTRACT: Alendronic acid modified resol nanocomposite resins (AA-PFNCRs) and sepiolite modified resol nanocomposite resins (SEP-PFNCRs) have been synthesized by *in situ* method in the presence of base catalyst. Additionally, the synergistic effects of alendronic acid and sepiolite clay (AA-SEP-PFNCR) on the resol resin have been studied. The structure, morphology, and thermal properties of these nanocomposites have been investigated by Fourier Transform Infrared Spectroscopy (FTIR), Differential Scanning Calorimetry (DSC), Thermogravimetric Analysis (TGA), and X-ray Diffraction (XRD). The results demonstrated the interactions between the fillers and resol resin. Thermal properties of nanocomposite resins were improved due to alendronic acid and sepiolite. The obtained samples were also characterized morphologically by Scanning Electron Microscope (SEM). © 2016 Wiley Periodicals, Inc. J. Appl. Polym. Sci. **2016**, *133*, 43807.

KEYWORDS: block copolymers; conducting polymers; polypyrroles; polysiloxanes; resins

Received 24 December 2015; accepted 17 April 2016
DOI: 10.1002/app.43807

INTRODUCTION

In polymer science, nanocomposites have received great attention as a result of performance improvements of polymers through the incorporation of nanosized fillers.[1] Typically, the main advantage is to enhance strength, stiffness, toughness, temperature resistance or dimensional stability by embedding particles in a matrix. Second advantage is to use cheap, readily available fillers to extend of scarce or expensive resin.

The nanometric size, its features, and the extraordinary high surface area of the dispersed clay are all related to the improvements in physical properties, such as tensile strength and modulus, gas permeability, lower coefficient of thermal expansion, and without changing the optical homogeneity of the material. In order to incorporate clay into a polymer matrix, different methods can be applied, such as solution intercalation, melt mixing, and *in situ* polymerization techniques. In these nanocomposites, not only significant improvement is gained in properties, but also enhancement in material processing, as well as reduction of component weight can be achieved. More polar groups in the polymer may enhance the ionic interaction between the polymer chains and the clays, leading to exhibit greater enhancement in physical-mechanical properties of the nanocomposites.

The immiscibility of clays with nonpolar polymers, namely PS, PE, PP, etc., may be overcome by treating clays with surfactant without adding compatibilizer, also discussed in this review. In addition, for *in situ* polymerized nanocomposites, the increased *d*-spacing allows using larger surfactant as clay modifier enables the monomer to penetrate into the gallery space and polymerize, resulting in improved reinforcement of the polymer matrix, as well as improvement of properties of the corresponding nanocomposites. Such features make the nanocomposites ideal candidates for a broad range of applications ranging from strong, heat resistant automotive components to high-barrier packaging materials, aerospace, optical, electronic, and medical devices.

Phenolic resins that are known as oldest synthetic polymers have been used commonly and they are among the most commonly used thermosetting resins. They are irreplacable materials for selective high-technology applications, offering high reliability under severe conditions. They have been widely used in the manufacture of wood products, coatings, structural adhesives, moulding compounds, composites, and thermal insulation materials. Most of these applications are due to their excellent thermal and chemical resistance and good dimensional stability.[2–6] A wood adhesive-type alkaline phenol formaldehyde resin

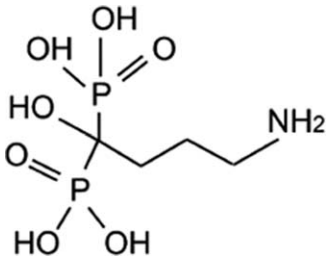

Figure 1. Structure of alendronic acid.

made with a phenol/formaldehyde charge ratio of 2.10 have been shown to reach a methylene/phenol ratio of between 1.35 and 1.46 when cured at elevated temperatures for ample periods of time, indicating that highly crosslinked polymer systems close to the structure described.[7]

On the other hand, phenolic resins have three-dimensional (3D) molecular structure even before curing, therefore the synthesis of phenolic resin nanocomposites is rather difficult. This situation limits the number of studies on these resins, compared to other thermosetting resins such as epoxy and unsaturated polyester.[7–11] Nevertheless, phenolic resin nanocomposites have attracted considerable attention in both scientific and industrial fields on account of their unexpected hybrid properties.[11]

Bisphosphonates (BPs) are synthetic compounds which includes P-C-P bridge. Among the bisphosphonates, (1-hydroxy-4-amino-butylidene)-1,1-bisphosphonic acid (or alendronic acid) is one of the most effective drugs used for the clinical treatment of bone diseases (Figure 1).[12–14] Additionally, the presence of phosphorus compounds has been reported in the literature to improve the flame retardancy and thermos-oxidative resistance of phenolic resins.[15–17] Ochiuz *et al.* investigated thermal stability of sodium alendronate (which is a monosodium salt of alendronic acid) in a mixture with crosslinked acrylic acid polymers and chitosan.[18] Önen *et al.* prepared ketonic resins that include alendronic acid, and used for synthesis of fire retardant polyurethane.[19]

Sepiolite is a fibrous hydrated magnesium silicate with the theoretical half unit-cell formula $Si_{12}O_{30}Mg_8(OH)_4(OH_2)_4{\cdot}8H_2O$. Its structure is similar to the 2:1 layered structure of MMT containing octahedral sheets of magnesium oxide/hydroxide sandwiched between two tetrahedral silica layers, except that the layers lack continuous octahedral sheets.[20,21] The structure of sepiolite is shown in Figure 2. Sepiolite shows an alternation of blocks and tunnels that grow up in the fibber direction. Each structural block is composed of two tetrahedral silica sheets sandwiching a central sheet of magnesium oxide-hydroxide (Figure 2).[22] This clay exhibits nanoneedle morphology with particle size over a wide range, however the dimensions of the fibres are generally 100–5000 nm length, 10–30 nm in width, and 5–10 nm in thickness. Furthermore, sepiolite has high surface area at the range of 200–300 m^2/g due to the presence of blocks and tunnels along the needle direction.[23,24]

The discontinuity of the silica sheets provides increasing of the silanol groups (Si-OH) at external surface of the sepiolite particles, which improves the interfacial interaction of sepiolite with organic solvent and polymers. As the presence of the tunnels and Si-OH, sepiolite can dispersed well in polymer matrix and thereby improve the mechanical properties, thermal stability, flame retardancy, and barrier properties of polymers.[25–27] In our previous work,[28] we synthesized *in situ* modified resol nanocomposites with different clay contents from 3 to 50 wt %. Considerable thermal stability enhancement of resol matrix has been found by incorporation of sepiolite due to the good dispersion and strong interfacial interaction between silanol groups of sepiolite and methylol groups of resol.

The purpose of this study is to obtain resol nanocomposites with the addition of alendronic acid as a nanoparticle to improve material properties. Furthermore, the synergist effects of alendronic acid and sepiolite clay were investigated. The nanocomposites were synthesized in one step via *in situ* method. Spectroscopic, thermal, and microscopic properties of the resin nanocomposite samples have been studied by Fourier Transform Infrared (FTIR-ATR) spectroscopy, Differential Scanning Calorimeter (DSC), Thermogravimetric Analyzer (TGA), and X-ray Diffraction (XRD).

EXPERIMENTAL

Materials

Phenol and sodium hydroxide pellets were purchased from Carlo Erba Reagents. Formaldehyde solution (37%), alendronic acid, and sepiolite clay were used from MERCK, Tolsa Group, and Chemos GmbH, respectively. All chemicals were used without further purification.

Synthesis

Synthesis of Neat Resol Resin (PFR). To synthesize PFR into a three-necked flask equipped with a mechanical stirrer, 0.2 mol

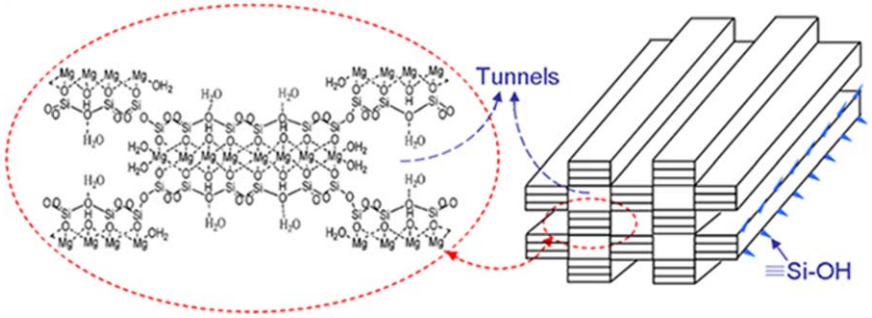

Figure 2. Crystalline structure and fiber structure of sepiolite clay. [Color figure can be viewed in the online issue, which is available at wileyonlinelibrary.com.]

of phenol and 0.4 mol of formaldehyde solution were added. To prevent the evaporation of mixture, a reflux condenser was installed the system. The mixture was stirred with mechanical stirrer for 4 h. Throughout the reaction, pH was adjusted to 9–10 using the 20 wt % NaOH solution and the temperature of oil bath was set to 85 °C. After 4 h, the liquid resin was transferred in a rotary evaporator under vacuum at 85 °C for 15 min to remove water that was formed during the reaction. At the end of rotary evaporation process, a very viscous resin was obtained that resembles a gel. The resin was dried in a vacuum oven at 100 °C hence solid resin was synthesized. Lastly, the solid resin was pulverized in a mortar to obtain powder form.

Synthesis of Sepiolite Modified Resol Resins (SEP-PFNCRs). SEP-PFNCRs were synthesized in two different initial sepiolite content by phenol weight (5 wt %, 10 wt %). At each polymerization, 0.2 mol (18.8 g) of phenol and 0.4 mol (33 mL) of formaldehyde solution were added into a three-necked flask. pH was adjusted to 10 using the 20 wt % NaOH solution and the temperature of oil bath was set to 85 °C. The mixture was stirred with mechanical stirrer for 4 h. For 3 and 5 wt % sepiolite contents, the resins were liquid therefore rotary evaporator used for removing water for 15 min at 85 °C in order to obtain a viscous resin. The other sepiolite samples (initial sepiolite content by phenol weight: 20–50 wt %) were very viscous thus rotary evaporation process was not applied. The viscous resin was dried in a vacuum oven at 100 °C and pulverized to powder.

Blank Experiment of Phenol Formaldehyde Resol–Sepiolite Resin. Blank experiment was done to prove the nanostructure of SEP-PFNCRs. Neat resol resin was synthesized as mentioned before. Then, 5 wt % of sepiolite clay was added and mixed with resol resin. After mixing, the precipitation of sepiolite clay was observed in resol resin. All of the *in situ* modified resol resins did not demonstrate phase separations, which verify the nanostructure.

Synthesis of Alendronic Acid Modified Resol Resins (AA-PFR). Two different alendronic acid weight ratios, which are 5 and 10 wt % of resol were used in synthesis. For the reaction, desired P/F molar ratio was 1/2 thus 0.2 mol (18.8 g) of phenol and 0.4 mol (33 mL) of formaldehyde solution were used. As a catalyst, NaOH solution (20 wt %) was added to the flask to fix the pH as 10. To prevent the evaporation, reflux condenser was installed to the system and oil bath temperature was adjusted to 85 °C. The reaction mixture was stirred for 4 h with mechanical stirrer for synthesizing the liquid resin. After this stage, rotary evaporator was used for removing water from the resin, which was formed during the reaction. Then, viscous resin was dried in the vacuum oven and pulverized.

Synthesis of Alendronic Acid and Sepiolite Modified Resol Resin (AA-SEP-PFNCR). AA-SEP-PFNCR was synthesized by the same method and by the same experiment setup. 18.8 g (0.2 mol) of phenol and 33 mL (0.4 mol) of formaldehyde solution and appropriate sepiolite (5 wt %) and alendronic acid (5 wt %) content by phenol weight were added into three-necked flask.

Characterization

FTIR analyses of samples were done with Nicolet 6700 FTIR-ATR reflectance spectrophotometer using OMNIC as software.

DSC measurements were performed with DSC 7020 Exstar. The cycle was heated from 30 to 250 °C with 10 °C/min heating rate.

Thermogravimetric analysis (TGA) was operated under nitrogen atmosphere by TG/DTA 7200 Exstar at a heating rate of 10 °C/min up 30–700 °C temperature.

XRD patterns were obtained with Rigaku D/Max-Ultima+/PC XRD instrument. Cu Kα radiation with a wavelength of $\lambda = 0.15406$ nm was applied in the range of 10–70°. Interlayer distance of resins calculated with Bragg equation ($n \cdot \lambda = 2 \cdot d \cdot \sin\theta$).

Morphology of products was examined by scanning electron microscope, ESEM XL30 ESEM-FEG Philips and the samples for the SEM measurement are prepared by gold coating.

RESULTS AND DISCUSSION

The alkaline phenol-formaldehyde (PF) resol resins are low molecular weight polycondensation products of phenol and formaldehyde obtainable in alkaline aqueous media. In cured PF resol resins, phenol molecules are linked by methylene groups in ortho- and para-carbons and also have hydroxymethyl groups bounded on other ortho- and para-carbons. Preparation of *in situ* modified phenol formaldehyde resin with alendronic acid and sepiolite was studied in the presence of base catalyst.

AA-PFNCRs, SEP-PFNCRs, and AA-SEP-PFNCR were synthesized via *in situ* method. Under alkaline conditions, the initial reaction product of phenol and formaldehyde is a mixture of ortho- and para-monohydroxy methylolated phenols. Resol is synthesized with excess formaldehyde, so more than one substitution can be seen on the phenol ring. Monohydroxymethyl-substituted phenols, react with formaldehyde to form di- and trihydroxymethyl-substituted phenols. Alendronic acid and sepiolite combine with the resol resin from their $-NH_2$ and Si–OH groups, respectively, by the effect of base-catalyzed condensation reactions.

Polymerization takes place by a methylol group connected to a phenol group reacting at the ortho- or para-position of another phenol group in order to form a methylene bridge that connects the two phenols. Dibenzyl ether bridges connecting two phenols are also formed by the reaction of two methylol groups with each other. With excess formaldehyde, methylol groups are formed on the terminal phenol groups of resol resins. The formation of nanocomposite resins was illustrated in Figures 3 and 4.

FTIR spectra of resin samples were recorded in the transmittance mode. The FTIR spectrum of PFR resin was shown in Figure 5. In this study, the characteristic peaks of PFR were observed at 3284, 2880, 1610, and 1479 cm^{-1} corresponded to the –OH groups, aliphatic C–H stretch, C=C aromatic ring vibrations, and CH_2 bending. Also, the absorbance at 1360, 1208, 1149, 1014, and 883 cm^{-1} were belonged to the OH plane deformation, phenolic C–O stretch, aromatic C–H, hydroxyl methyl C–O stretch, and o,p – o,o', p-substituted phenol,

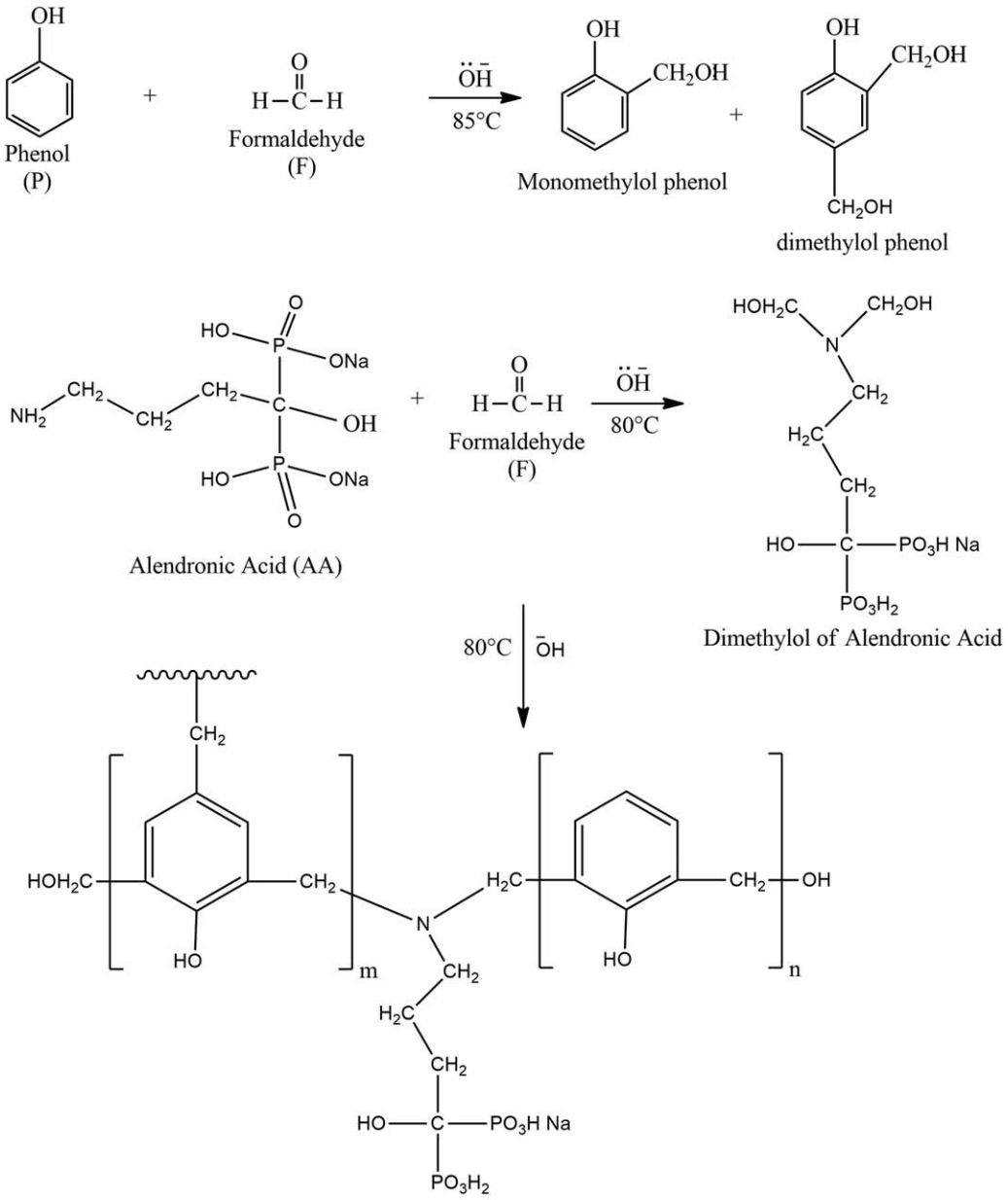

Figure 3. Synthesis of AA-PFNCRs.

respectively, while the peaks at 823 and 753 cm^{-1} corresponded to p-substituted and o-substituted phenol.

To synthesize AA-PFNCRs, SEP-PFNCRs, and AA-SEP-PFNCR, alendronic acid and sepiolite were added to the reaction mixture. Therefore, the FTIR spectrum of neat sepiolite and alendronic acid spectrums were given in Figures 6 and 7 for comparison.

From Figure 6, the peaks at 3561 and 644 cm^{-1} are from Mg–OH stretching and Si–O–Si vibrating of sepiolite, and the biggest peaks at 1005 and 974 cm^{-1} are the Si–O and Si–O–Si vibrating of neat clay. In alendronic acid spectrum strong bands in the region 1200–900 cm cm^{-1} correspond to C–O and P═O stretches (Figure 7).

As shown in Figure 8 in addition to the characteristic peaks of PFR, Si–O–Si vibrating peak of sepiolite, C–O and P═O stretches of alendronic acid were also seen in samples. The intensity of sepiolite and alendronic acid peaks strengthened with increasing amount of fillers in the nanocomposites and the intensity of resol peaks (–OH) have decreased.

Thermal behavior of resins was examined by differential scanning calorimetry (DSC) in the range of 30–250 °C and by TGA in the range of 30–900 °C. Differential scanning calorimetry (DSC) was used to measure the temperatures and heat flows associated with exothermic and/or endothermic changes that occur during thermal transitions of the samples. The measurements of AA5%-PFNCR, AA10%-PFNCR, SEP5%-PFNCR, SEP10%-PFNCR, and

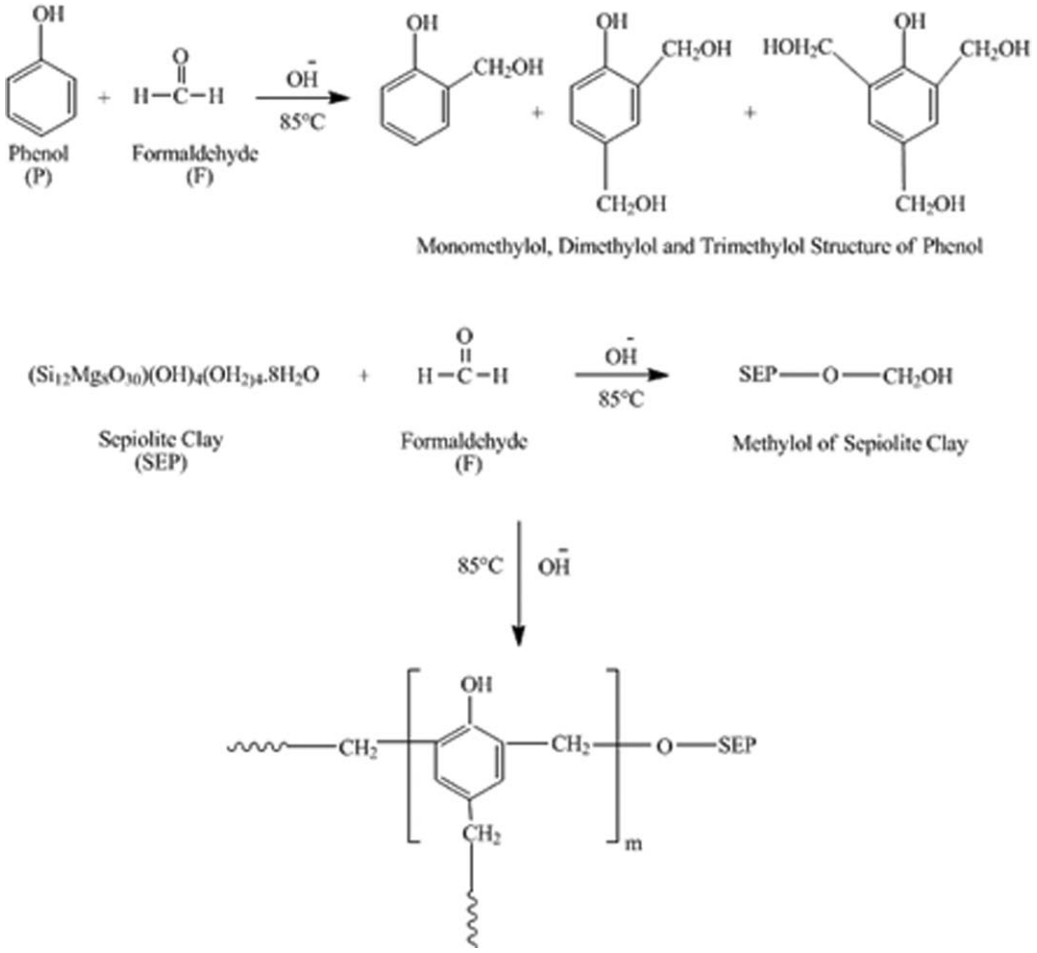

Figure 4. Synthesis of SEP-PFNCRs.

AA5%-SEP5%-PFNCR were operated with one cycle. The cycle was heated from 30 to 200 °C with 10 °C/min heating rate.

The main application of DSC for phenolic resins is the specification of maximum cure temperatures and onset of cure temperatures. The technique is very useful when examining the effect of processing changes on cure. The determination of maximum cure temperatures and onset of cure temperatures of SEP5%-PFNCR was given in Figure 9. The overall results in Table I. Changes in the percent of sepiolite clay and alendronic acid affected the onset of cure temperature and maximum cure temperature. According to the results, the exothermic maximum cure temperature peak was found to be between 171 and 196 °C. On the other hand, DSC results showed the synergist effect of alendronic acid and sepiolite clay. AA5%-SEP5%-PFNCR had higher temperature values than AA5%-PFNCR and SEP5%-PFNCR that offers the combination of these materials.

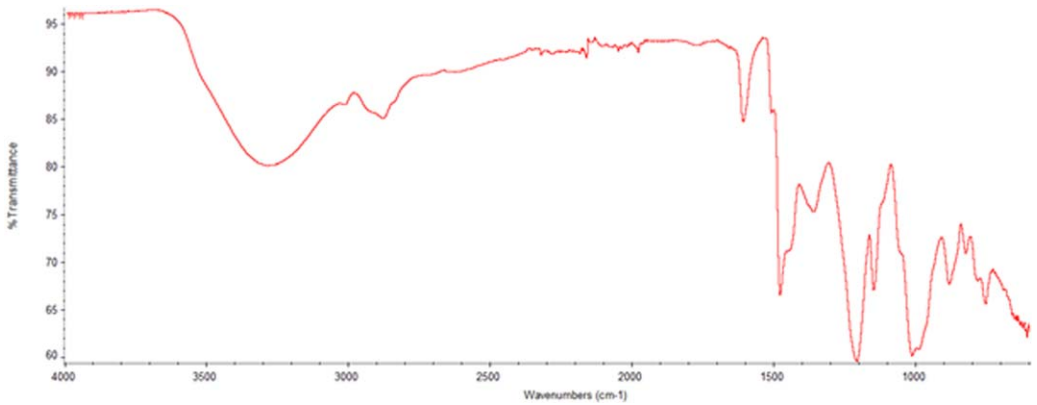

Figure 5. FTIR spectrum of PFR. [Color figure can be viewed in the online issue, which is available at wileyonlinelibrary.com.]

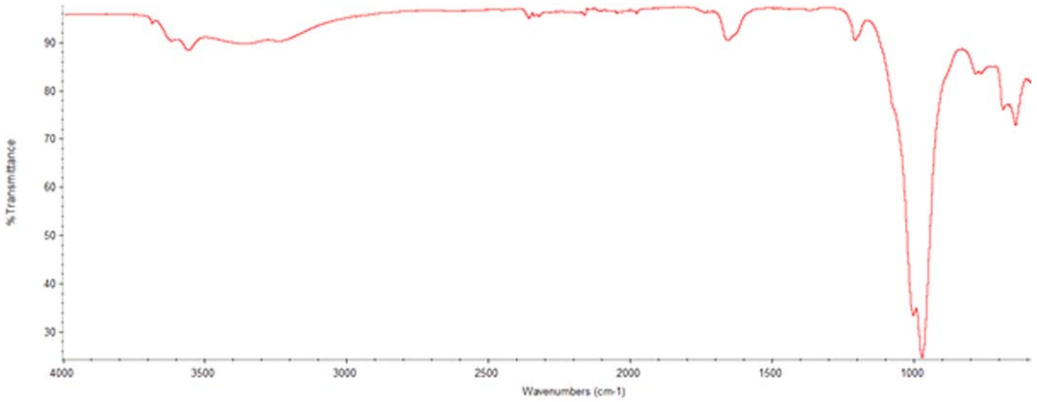

Figure 6. FTIR spectrum of sepiolite clay. [Color figure can be viewed in the online issue, which is available at wileyonlinelibrary.com.]

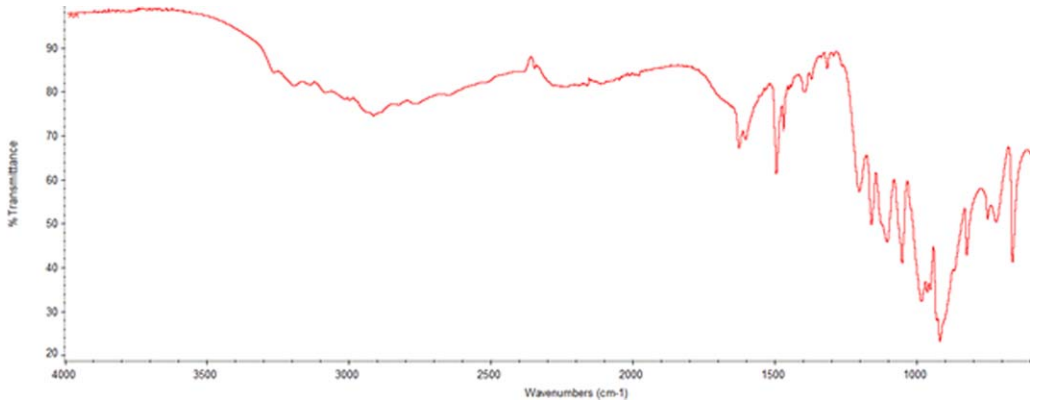

Figure 7. FTIR spectrum of alendronic acid. [Color figure can be viewed in the online issue, which is available at wileyonlinelibrary.com.]

Thermal decomposition behaviors of PFR, AA-PFNCRs, SEP-PFNCRs, and AA-SEP-PFNCR samples were determined with TGA measurements. In order to prepare TGA samples, resol resin and the nanocomposite resol resins were partially cured at 100 °C for 1 h. Degradation was carried out in nitrogen gas to the maximum temperature of 700 °C. The weight loss (wt %) of the resins was calculated, the weight loss (%) rates were shown as a function of temperature in Figure 10 and Table II. Different stages of degradation were seen in the TGA thermogram (Figure 10): the first stage (150 °C), the second stage (250–350 °C) and the third stage (350–700 °C). Onset temperature of degradation (°C) and residue amount (%) at 700 °C were calculated and these values are given in the Table II. In the first stage, of thermal decomposition was water lost from methylol groups of nanocomposite resins. In the second stage, the release of formaldehyde occurred due to break of ether bridges and methylene bridges were broken. The last and third stage of decomposition, oxidation of the network occurred. At 700 °C, the all residues

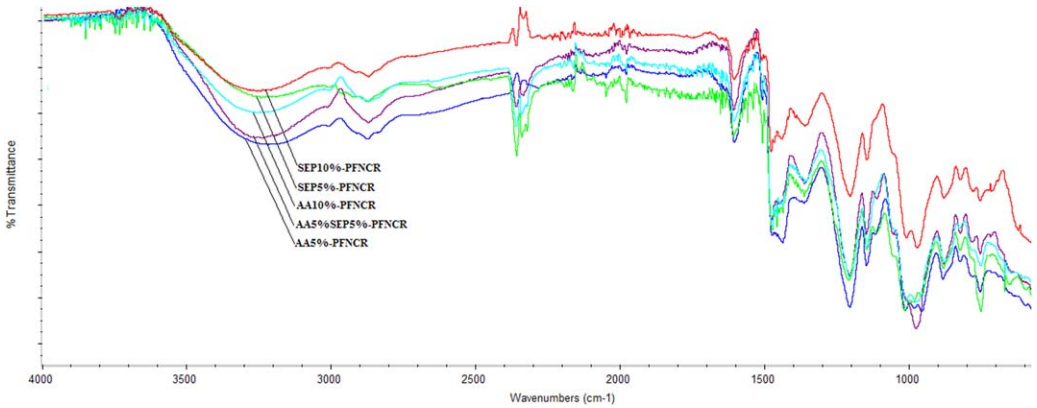

Figure 8. FTIR spectra of AA-PFNCRs, SEP-PFNCRs, and AA-SEP-PFNCR. [Color figure can be viewed in the online issue, which is available at wileyonlinelibrary.com.]

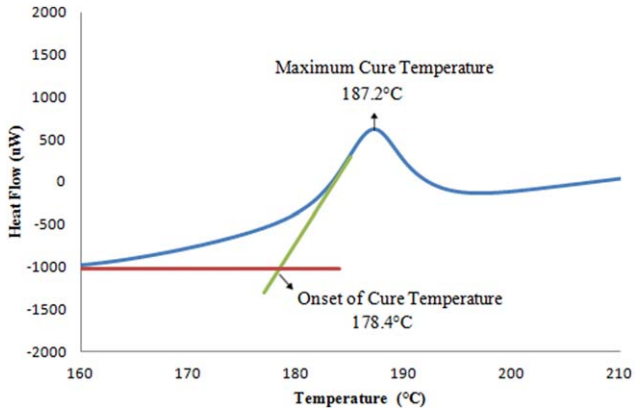

Figure 9. Determination of the maximum cure temperature and onset of cure temperature for SEP5%-PFNCR from DSC plot. [Color figure can be viewed in the online issue, which is available at wileyonlinelibrary.com.]

Table I. DSC Results of Samples

Sample	Maximum cure temperature (°C)	Onset of cure temperature (°C)
AA5%-PFNCR	171.4	163.0
AA10%-PFNCR	187.3	178.0
AA5%-SEP5%-PFNCR	192.7	182.4
SEP5%-PFNCR	187.2	178.4
SEP10%-PFNCR	196.0	185.2

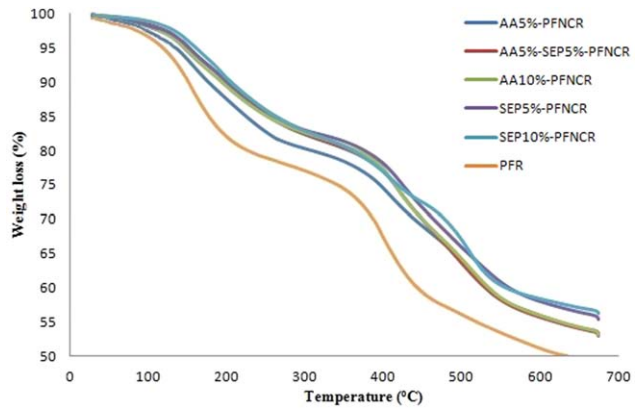

Figure 10. TGA thermograms of PFR and nanocomposite resins. [Color figure can be viewed in the online issue, which is available at wileyonlinelibrary.com.]

Table II. TGA Results of Samples

Sample	Onset temperature of degradation (°C)[a]	Residue (%) at 700 °C[a]
PFR	113.6	47
AA5%-PFNCR	122.7	53
AA10%-PFNCR	125.6	54
AA5%-SEP5%-PFNCR	129.2	54
SEP5%-PFNCR	128.3	56
SEP10%-PFNCR	132.5	57

[a] Detected by TGA.

Table III. Diffraction Characteristics of Samples

Sample	2θ (°)	*d*-spacing (nm)
PFR	21.48	0.413
SEP	7.46	1.184
AA5%-PFNCR	19.62	0.452
AA10%-PFNCR	3.28	2.693
AA5%-SEP5%-PFNCR	7.82	1.130
SEP5%-PFNCR	7.38	1.196
SEP10%-PFNCR	7.42	1.190

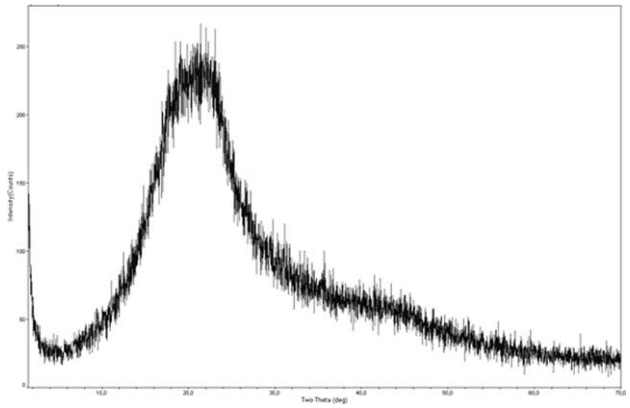

Figure 11. XRD pattern of PFR.

are above the 50%, so that the thermal stability of specimens was enhanced.

As demonstrated in Figure 10 and Table II as the percent of alendronic acid doubled, the residue of alendronic acid content was slightly increased (AA5%-PFNCR and AA10%-PFNCR). On the other hand, the thermal stability of SEP5%-PFNCR was found to be greater than AA5%-PFNCR. Therefore, sepiolite has better thermal effects than alendronic acid. Furthermore, AA5%-SEP5%-PFNCR had same residue with AA10%-PFNCR.

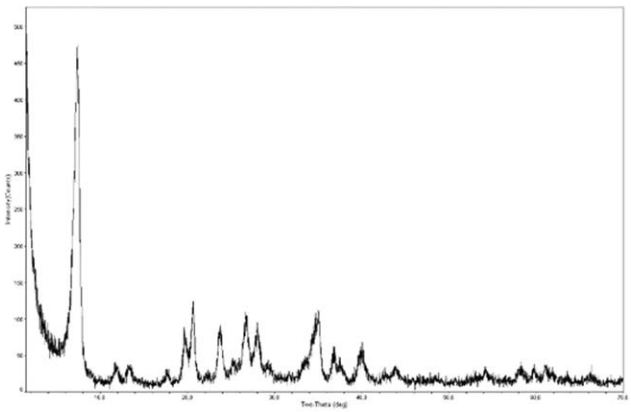

Figure 12. XRD pattern of SEP.

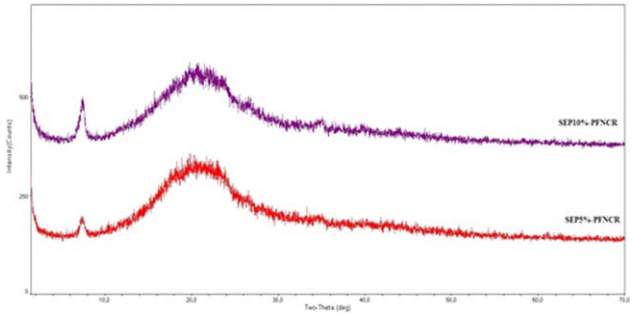

Figure 13. XRD graph of SEP-PFNCRs. [Color figure can be viewed in the online issue, which is available at wileyonlinelibrary.com.]

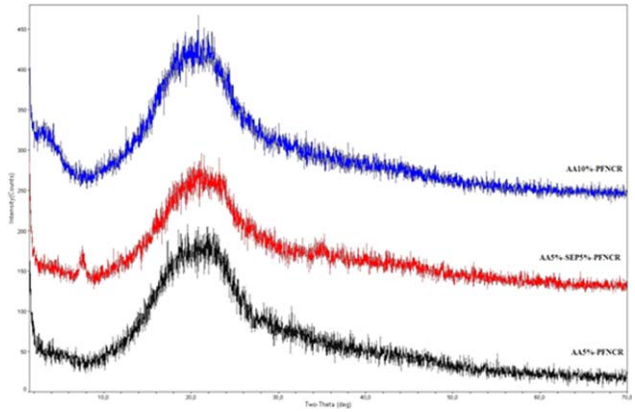

Figure 14. XRD graph of AA-PFNCRs and AA-SEP-PFNCR. [Color figure can be viewed in the online issue, which is available at wileyonlinelibrary.com.]

The structures and the variations of spacing of the neat resol and modified resol resins were detected by X-ray diffraction. In Table III, *d*-spacing's (nm), which was calculated by Bragg's Equation ($n\cdot\lambda = 2\cdot d\cdot\sin\theta$), and 2θ angles are shown.

The 2θ value and *d*-spacing of the neat PFR used were found to be 21.48° and 0.413 nm (Figure 11 and Table III). For sepiolite clay, the values were determined as 7.46° and 1.184 nm, respectively (Figure 12 and Table III). XRD graph of sepiolite modified resol resins were given Figure 13. The values of PFR and sepiolite are compatible with the results of the literature.[22,29,30]

The diffraction patterns of the resols pre-Þred at temperatures below 500 °C show a single halo at about 20°, being essentially similar to that of unÞred sample.[31]

The XRD pattern of the AA5%-PFNCR had only one peak close to that of the pristine polymer (Figure 14). This suggests that alendronic acid particles were well exfoliated and dispersed

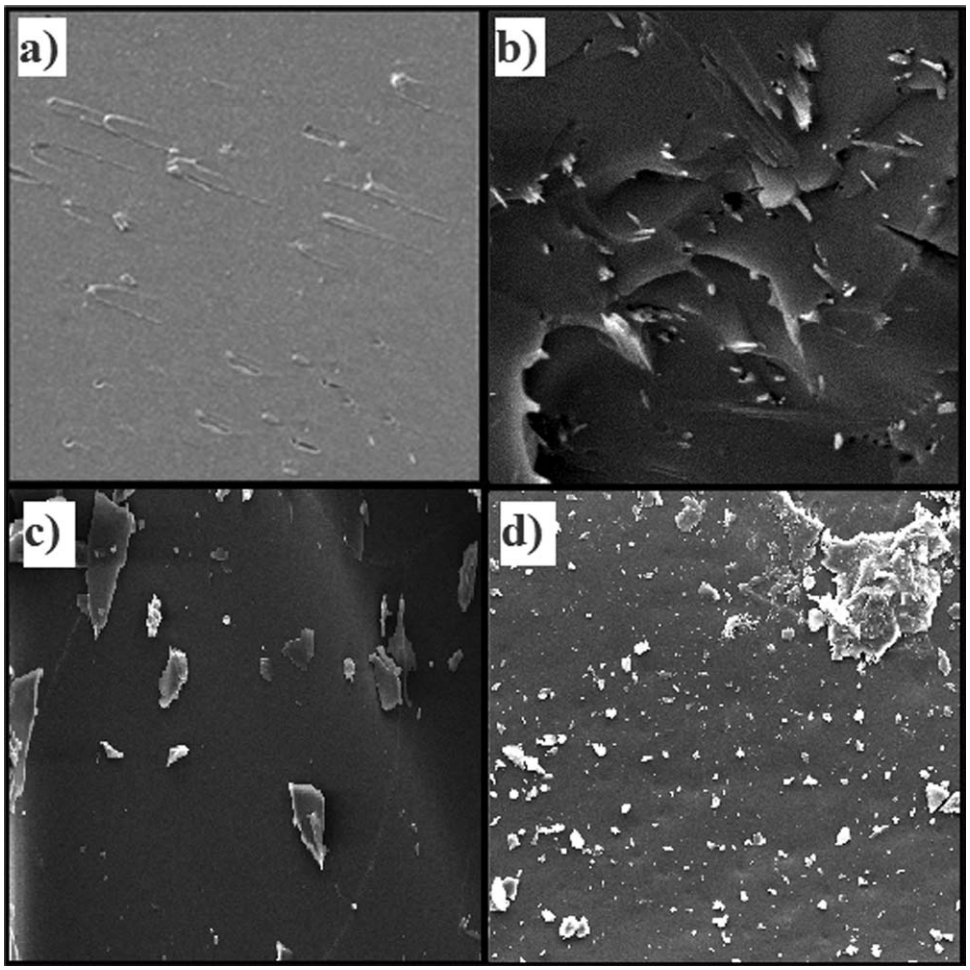

Figure 15. SEM images of (a) PFR (2000×), (b) SEP10%-PFNCR (1000×), (c) AA5%-PFNCR (1000×), (d) AA5%-SEP5%-PFNCR (1000×).

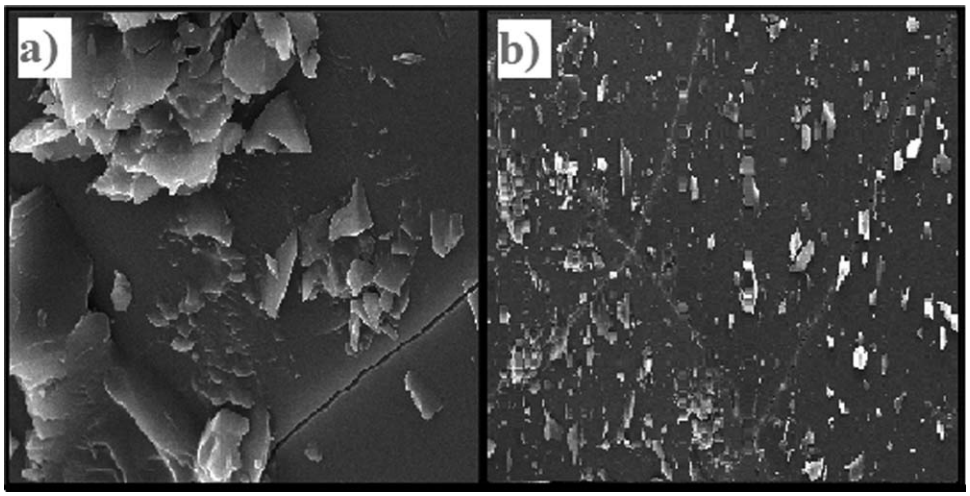

Figure 16. SEM images of (a) AA10%-PFNCR (10,000×) and (b) AA10%-PFNCR (1000×).

uniformly in the polymer matrix. The *d*-spacing of AA5%-PFNCR was slightly increased compared to PFR. On the other hand, the nanocomposite AA10%-PFNCR had a slight of alendronic acid peak at 3.28°. This result confirms that the alendronic acid dispersion at a higher content has a tendency of intercalated structure. Following the addition of the sepiolite clay to neat resol, the samples of SEP5%-PFNCR and SEP10%-PFNCR have the intense diffraction peak, visible in the nanocomposites corresponding to the channel reflections of the sepiolite structure, therefore proving the intercalated structure. AA5%-SEP5%-PFNCR has a sepiolite peak at 7.82° and the interlayer distance was found as 1.130 nm. The value is lower than SEP5%-PFNCR because of the presence of alendronic acid.

SEM images of PFR, SEP10%-PFNCR, AA5%-PFNCR, AA5%-SEP5%-PFNCR, and AA10%-PFNCR were shown in Figures 15 and 16, respectively. As it is seen in figures, embedded nanoclay particles can be seen on the sample surfaces. With magnification 1000× homogeneous dispersion of clay and alendronic acid particles can be seen. Homogen dispersing of nanoparticles was smoothly achieved for samples with clay contents of 5 and 10 wt % (Figure 15). But above the content of 10 wt %, as seen in the Figure 16 agglomeration of alendronic acid particles occurred.

CONCLUSIONS

In this article, the individual and synergist effects of alendronic acid and sepiolite clay were studied via *in situ* method. The FTIR studies were carried out to understand the interactions between resol, alendronic acid, and sepiolite. According to FTIR analysis, the peaks of alendronic acid and sepiolite are observed in the spectrums, therefore successful synthesis of the nanocomposites was confirmed.

The determination of maximum cure temperatures and onset of cure temperatures of samples was performed with DSC. The increasing of onset of cure temperature and maximum cure temperature was correlated with the enhancement of sepiolite and alendronic acid percentages. The DSC results of AA5%-SEP5%-PFNCR were found to be better than the AA5%-PFNCR and SEP5%-PFNCR. This suggests the combination of these materials. With TGA analysis, a considerable thermal stability enhancement has been found for resol matrix. The residue of samples was found to be above the 50% of initial sample at 700 °C. When the influence of the alendronic acid and sepiolite was compared, sepiolite certainly had better resistance.

According to XRD results, AA5%-PFNCR had exfoliated structure, and with increasing alendronic acid content, intercalated structure obtained for AA10%-PFNCR. Furthermore, the results have showed the intercalated structure of SEP-PFNCRs. In conclusion, clay particles were successfully dispersed in resol resin matrix and nanocomposites resins with better thermal properties were obtained which can be used for thermal insulation materials, coatings, molding compounds, and aerospace components.

ACKNOWLEDGMENTS

This work was financially supported by Istanbul Technical University Research Foundation (İTÜ-BAP Project No: 38362).

REFERENCES

1. Yilgor, E.; Eynur, T.; Kosak, C.; Bilgin, S.; Yilgor, I.; Malay, O.; Menceloglu, Y.; Wilkes, G. L. *Polymer* **2011**, *52*, 4189.
2. Zmihorska-Gotfryd, A. *Prog. Org. Coatings* **2004**, *49*, 109.
3. Hsief, F.; Beeson, H. D. *Fire Mater.* **1997**, *21*, 41.
4. Pilato, L. *React. Funct. Polym.* **2013**, *73*, 270.
5. Astarloa-Aierbe, G.; Echeverria, J. M.; Vazquez, A.; Mondragon, I. *Polymer* **2000**, *41*, 3311.
6. Fang, Q.; Cui, H.; Du, G. *Int. J. Adhes. Adhes.* **2014**, *49*, 33.
7. Kim, M. G.; Wu, Y.; Amos, L. W. *J. Polym. Chem. Sci. Part A* **1997**, *35*, 3275.
8. Lopez, M.; Blanco, M.; Vazquez, A.; Gabilondo, N.; Arbelaiz, A.; Echeverria, J. M.; Mondragon, I. *Thermochim. Acta* **2008**, *467*, 73.

9. Lopez, M.; Blanco, M.; Martin, M.; Mondragon, I. *Polym. Eng. Sci.* **2012**, *52*, 1161.
10. Kaynak, C.; Tasan, C. C. *Eur. Polym. J.* **2006**, *42*, 1908.
11. Özkaraman, G.; Kızılcan, N. *J. Appl. Polym. Sci.* **2013**, *129*, 2966.
12. Boanini, E.; Gazzano, M.; Rubini, K.; Bigi, A. *Adv. Mater.* **2007**, *19*, 2499.
13. Rogers, M. *J. Curr. Pharm. Des.* **2003**, *9*, 2643.
14. Russell, R. G.; Rogers, M. *J. Bone* **1999**, *25*, 97.
15. Gardziella, A.; Pilato, L. A.; Knop, A. Phenolic Resins: Chemistry, Applications, Standardization, Safety and Ecology, 2nd ed.; Springer-Verlag: Berlin, **2000**.
16. Nair, C. P. R. *Prog. Polym. Sci.* **2004**, *29*, 401.
17. Abdalla, M. O.; Ludwick, A.; Mitchell, T. *Polymer* **2003**, *44*, 7353.
18. Ochiuz, L.; Lisa, G.; Grigoras, C.; Avadanei, M.; Gafitanu, E. *Mater. Plast.* **2008**, *45*, 372.
19. Önen, D.; Kızılcan, N.; Yıldız, B.; Akar, A. *Int. J. Chem. Nucl. Mater. Metall. Eng.* **2015**, *9*, 234.
20. Sandi, G.; Winans, R. E.; Seifert, S.; Carrado, K. A. *Chem. Mater.* **2002**, *14*, 739.
21. Zotti, A.; Borriello, A.; Martone, A.; Antonucci, V.; Giordano, M.; Zarrelli, M. *Composites Part B* **2014**, *67*, 400.
22. Chen, H.; Zheng, M.; Sun, H.; Jia, Q. *Mater. Sci. Eng. A* **2007**, *445–446*, 725.
23. Duquesne, E.; Moins, S.; Alexandre, M.; Dubois, P. *Macromol. Chem. Phys.* **2007**, *208*, 2542.
24. Kuang, W.; Facey, G. A.; Detellier, C. *Clays and Clay Miner.* **2004**, *52*, 635.
25. Yu, Y.; Qi, S.; Zhan, J.; Wu, Z.; Yang, X.; Wu, D. *Mater. Res. Bull.* **2011**, *46*, 1593.
26. Lopez, D. G.; Fernandez, J. F.; Merino, J. C.; Santaren, J.; Pastor, J. M. *Compos. Sci. Technol.* **2010**, *70*, 1429.
27. Cho, H. J.; Park, S.; Ha, C. S. *Polym. Int.* **2014**, *64*, 96.
28. Alkan, ÜB.; Kızılcan, N. *Procedia-Social Behav. Sci.* **2015**, *195*, 2067.
29. Spurr, R. A.; Erath, E. H.; Myers, H. *Ind. Eng. Chem.* **1957**, *49*, 1838.
30. Soheilmoghaddam, M.; Wahit, M. U.; Yussuf, A. A.; Al-Saleh, M. A.; Whye, W. T. *Polym. Test.* **2014**, *33*, 121.
31. Onodera, A.; Terashima, K.; Urusushihara, T.; Suito, K. *J. Mater. Sci.* **1997**, *32*, 4309.